Energy-Based Adaptive Sliding Mode Speed Control for Switched Reluctance Motor Drive System

M. M. Namazi Isfahani*, A. Rashidi* and S. M. Saghaian-Nejad*

Abstract: Torque ripple minimization of switched reluctance motor drives is a major subject based on these drives' extensive use in the industry. In this paper, by using a well-known cascaded torque control structure and taking the machine physical structure characteristics into account, the proposed energy-based (passivity-based) adaptive sliding algorithm derived from the viewpoint of energy dissipation, control stability and algorithm robustness. First, a nonlinear dynamic model is developed and decomposed into separate slow and fast passive subsystems that are interconnected by negative feedbacks. Then, an outer loop speed control is employed by adaptive sliding controller to determine the appropriate torque command. Finally, to reduce torque ripple in switched reluctance motor a high-performance passivity-based current controller is proposed. It can overcome the inherent nonlinear characteristics. The performance of the proposed controller algorithm has been demonstrated in simulation, and experimental using a 4KW, four-phase, 8/6 pole SRM DSP-based drive system.

Keywords: Feedback Dissipative Hamiltonian Realization (FDHR), Passivity-Based Control (PBC), Switched Reluctance Motor (SRM), Torque Ripple Minimization.

1 Introduction

In recent years, there is a growing concern in use of switched reluctance motor. The major reasons for SRM are robustness, high efficiency, low cost, high speed, simple structure, easy to maintain, high controllability, high torque to inertia ratio, simple power converter circuits with reduced number of switches and smaller dimension of the motor in comparison to the other motors [1]. The main problems with SRM include high torque pulsation and noise. Several control methods and schemes have been proposed to overcome these problems. For example, variable structure controller made the SRM drive system insensitive to parameter variations and load disturbance [2]. Artificial neural network and fuzzy controller needs a lot of designer experience [3]. Nonlinear internal model control for SRM drive required very complicated computations and implementation of the system is very difficult [4]. Some studies have succeeded in torque ripple reduction of SR motors using DTC method [5]. In the methods mentioned above, controller design procedure only done for speed or torque tracking and just speed loop as an outer loop is considered and the current loop is neglected. However, the torque is usually controlled via an inner current loop, with a nonlinear relationship between torque and current. That means the torque ripple, acoustic noise, speed performance and motor efficiency will be fractional affected by improving the current control. Also, for the above-mentioned control strategies of the SRM it is assumed that its parameters are known exactly or the unknown parameters can be identified by the adaptive technique. However, the parameters of the SRM are not exactly known and always vary with current and position. Actually, control is difficult to implement owing to its complex algorithm when considering the structural information of SRM in design. Improving the applicability of the SRM on the basis of taking the structural characteristics into account is a significant step in designing the controller of the SRM. In this paper, a cascaded torque control structure for its well-known advantages is used. First an adaptive sliding mode controller for speed loop control is designed and then compared to a PI controller. Then to achieve high performance torque control a nonlinear feedback current controller using energy-based technique called passivity-based control (PBC) theory which effectively uses the natural energy dissipation properties of the SRM, is proposed. PBC, introduced to define an energy-based nonlinear controller design methodology which achieves stabilization by

Iranian Journal of Electrical & Electronic Engineering, 2012.
Paper first received 14 May 2011 and in revised form 8 Oct. 2011.
* The Authors are with the Department of Electrical and Computer Engineering, Isfahan University of Technology, Isfahan, Iran.
E-mails: mm.namazi@ec.iut.ac.ir, 315.amir@gmail.com and saghaian@cc.iut.ac.ir.

passivation [6]. The algorithms is first simulated by MATLAB/SIMULINK and then tested experimentally on a four-phase 8/6 pole 4kW oulton SRM.

2 Nonlinear Construction and Modeling of SRM

Owing to the doubly salient construction, the SRM presents a highly nonlinear load to the current controller, thus the design of a high-performance current controller for an SRM drive is a challenge [7]. For SRM drives, the mutual coupling between phases is usually neglected for low-speed applications, so the phase currents can be controlled independently. Voltage equation for one phase of an SRM is [8]:

$$v_k = r_k i_k + \frac{d\lambda_k(\theta, i_k)}{dt}$$
$$= r_k i_k + L_k(\theta, i_k)\frac{di_k}{dt} + \frac{\partial \lambda_k(\theta, i_k)}{\partial \theta}\omega \qquad (1)$$

where u_k is the phase voltage, i_k is the phase current, r_k is the phase resistance, $k = a, b, c, d$ is the active phase, θ is the rotor position and $\lambda_k(\theta, i_k)$ is the flux linkage, $L_k(\theta, i_k) = \partial \lambda_k(\theta, i_k)/\partial i_k$ is the incremental inductance, $\omega = d\theta/dt$ is the motor speed and $e = \omega.\partial \lambda_k(\theta, i_k)/\partial \theta$ is the back EMF. Fig. 1 (a) and (b) shows the experimentally measured static flux linkage and torque characteristics of a four-phase 8/6 SRM whose parameters are specified in the Table 1 (in the Appendix) and used in this investigation. Using numerical methods, the incremental inductance and back-EMF characteristics of the SRM can be obtained from the measured flux linkage data. Fig. 1(c) and 1(d) shows the curves of calculated incremental inductance and back-EMF coefficient ($\partial \lambda_k(\theta, i_k)/\partial \theta$) against rotor position and phase current. Both incremental inductance and back-EMF coefficient are nonlinear functions of rotor position and phase current.

3 The Proposed Nonlinear Controller Design

In this section, we present a passivity-based adaptive sliding mode control method for designing SRM controller. A complete model of an SRM possesses two-time-scale characteristics and can be decomposed as the feedback interconnection of the two linked subsystems (electrical and mechanical subsystem) [9]. Also, in [10] it is proven that these two subsystems are passive linked subsystems as:

$$\text{electrical subsystem}: \quad \begin{bmatrix} v_k \\ -\dot{\theta} \end{bmatrix} \mapsto \begin{bmatrix} i_k \\ T_e \end{bmatrix} \qquad (2)$$
$$\text{mechanical subsystem}: \quad (T_L - T_e) \mapsto -\dot{\theta}$$

The overall control block diagram, shown in Fig. 2 is separated into the inner loop and the outer loop controller. Based on the assumption that stator current

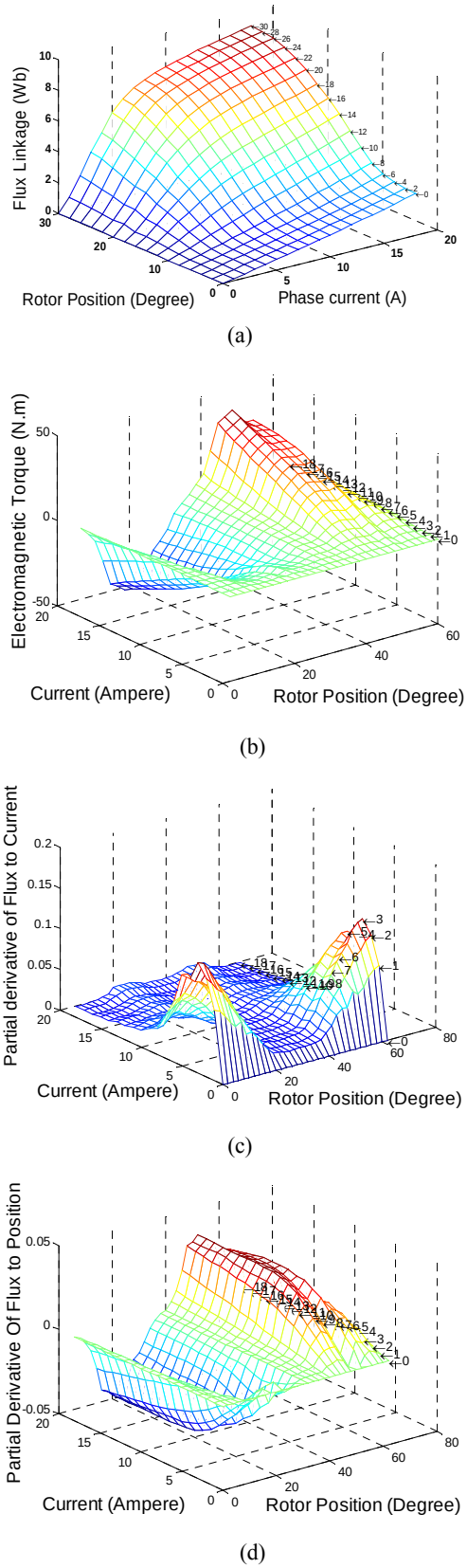

Fig. 1 Nonlinear characteristics of tested 8/6 SRM. (a) Measured Flux linkage. (b) Measured Torque. (c) Calculated incremental inductance. (d) Calculated back EMF coefficient.

i_k as well as rotor speed ω are available for measurement, controller design procedures can be divided into three steps. First step is to design an adaptive sliding speed controller for speed tracking of the overall system. The next step is passivity-based current control of the electrical subsystem by injecting a nonlinear electrical damping term and a set of reference current vectors i_k^* are found out to achieve current tracking. The sake of the outer loop is to generate the appropriate torque command fed for the inner loop. Finally, passivity-based inner loop current controller will produce the appropriate switching functions.

3.1 Speed Loop Controller Design

A sliding mode control scheme is proposed for the speed control and then compared to PI controller. The conventional adaptive sliding mode control estimates the unknown uncertainty upper boundary which causes the chattering phenomenon. Therefore, a method has been adapted to estimate the unknown uncertainties of lump without using sgn(·) that it reduces chattering [11]. For speed controller design, consider the mechanical equation $\dot{\omega} = (1/J)\left[T_e(\theta, i_k) - T_L - D\omega\right]$ with uncertainties as:

$$\frac{d\omega}{dt} = (a + \Delta a)\omega + (b + \Delta b)(T_e - T_L) \tag{3}$$

where $a = -B/j, b = 1/j$. Defining the state variable of speed error as $e = \omega^* - \omega$, switching surface as $S_d = \sigma e + \dot{e}$, $x = \left[x_1 \quad x_2\right]^T = \left[e \quad \ddot{\omega}\right]^T$ and choosing Lyapunov function as $V_1 = 1/2 S_d^2$, we have:

$$\begin{aligned} \dot{V}_1 &= S_d \dot{S}_d \\ &= S_d\left[-(\sigma + a)\dot{\omega} - bu + b\dot{T}_L\right] - b(\tilde{P} + \hat{P}) \end{aligned} \tag{4}$$

Where

$$P(t) = 1/b\left[\Delta a \cdot \omega + \Delta b(\dot{T}_e - \dot{T}_L)\right]; \tilde{P}(t) = P(t) - \hat{P}(t)$$

The estimated value of the lumped uncertainty is $\hat{P}(t)$ and $\tilde{P}(t)$ is the estimated error between the actual value $P(t)$ and the estimated value of the lumped uncertainty. Therefore, the new candidate function is $\dot{V}_2 = 0.5\left(S_d^2 + (1/\rho)\tilde{P}^2\right)$, then we have

$$\begin{aligned} \dot{V}_2 &= S_d\left[-(\sigma + a)\dot{\omega} - b(u + \hat{P}) + b\dot{T}_L + K_1 S_d\right] \\ &\quad - \tilde{P}\left(\frac{1}{\rho}\dot{\hat{P}} + bS_d\right) - K_1 S_d^2 \end{aligned} \tag{5}$$

If control input *u* is chosen as:

$$u = \frac{1}{b}\left[-(\sigma + a)\dot{\omega} - b\hat{P} + b\dot{T}_L + K_1 S_d\right] \tag{6}$$

One can obtain $\dot{V}_2 = -K_1 S_d^2 \le 0$ and it can be achieved that $\int_0^t W(\tau)d\tau = V\left[S_d(t)\right] - V\left[S_d(0)\right]$. Since $S_d(t)$ and $S_d(0)$ are bounded, according to Barbalet lemma [12], can be obtained that $\lim_{t\to\infty} W(\tau) = 0$. It means that $e \to 0$ as $t \to \infty$ and as a result, the proposed SRM drive system is stable. Finally in this step a proportional-integral (PI) controller is designed here to compare with the nonlinear controller. The parameters of the PI controller are tuned by pole placement [13]. By assumption of $\xi = 1.25$ and $\omega_n = 0.7 \text{ rad/sec}$ the parameters of the PI controller obtained as $K_P = 0.466$, $K_I = 7.47$.

3.2 Passivity-Based Current Control Design using Feedback Dissipative Hamiltonian Realization

As mentioned in previous section the electrical subsystem is passive. Therefore, in this section the feedback dissipative Hamiltonian realization method for passivity-based current controller design of SRM is proposed. Control design procedures can be divided into two steps. First, a suitable control that transfers dynamic model to a dissipative Hamiltonian system is fined. Finally, this section presents the PBC technique and then the current control law obtained. The feedback dissipative Hamiltonian realization method considers the problem of designing a state-space controller for the stabilization of a desired equilibrium point of a nonlinear system [14]:

$$\dot{x} = f(x) + g(x)u \tag{7}$$

where $x \in R^n$ are system states, $u \in R^m$ are system inputs. System (7) is said to have a feedback Hamiltonian realization if there exists a control law $u = \varphi(x)$, Such that the closed loop is of the form:

$$\dot{x} = F_d(x)\frac{\partial}{\partial x}H_d(x) \tag{8}$$

System (7) is said to have a feedback dissipative Hamiltonian realization if the closed loop is a dissipative Hamiltonian system, its structure matrix satisfies:

$$F_d(x)^T + F_d(x) \le 0 \tag{9}$$

where $F_d \in R^{(n)\times(n)}$ are called the structure matrices and $H_d(x)$ the Hamiltonian function. The key idea behind the technique is to match the closed-loop dynamics to a port-controlled Hamiltonian system form:

$$f(x) + g(x)u = F_d(x)\partial H_d(x) \tag{10}$$

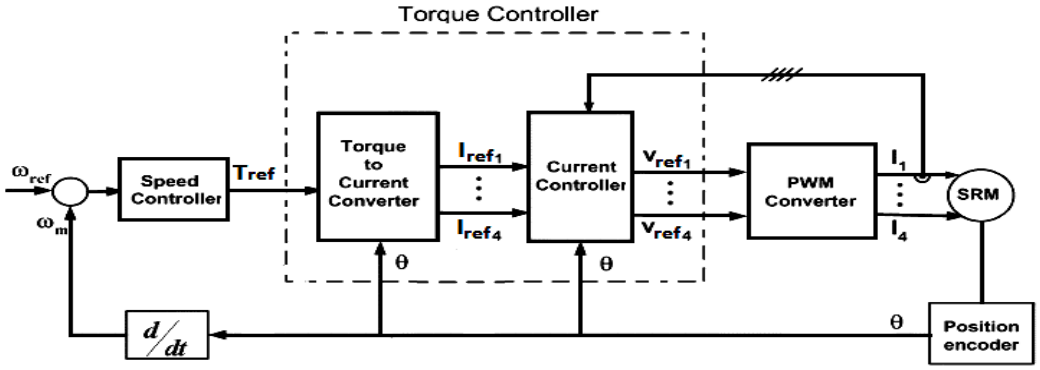

Fig. 2 The closed-loop SRM drive system based on current control strategy

To enforce dissipativity, the constraint of (9) on the F_d matrix is required. In this case, F_d decomposed as $F_d(x) = J_d(x) - R_d(x)$. The interconnection structure is captured in the matrix $J_d(x) = -J_d^T(x)$. The dissipation effects are captured by the matrix $R_d = R_d^T \geq 0$. In general, this leads to a set of partial differential equations. But for a real physical system, according to its physical meaning and the control objectives, we may find a natural candidate Hamiltonian function, then (9) becomes a set of algebraic equations.

Lemma 1: Necessary and sufficient condition for the existence of feedback dissipative Hamiltonian realization for fixed $F_d(x)$, which satisfy (10), and for fixed Hamiltonian function $H_d(x)$, is that there exists a feedback such that (10) holds if and only if the projected matching equation:

$$g^{\perp}(x)\left(f(x) - F_d(x)\partial H_d(x)\right) = 0 \tag{11}$$

Holds for an arbitrary full-rank left annihilator $g^{\perp}(x)$. By defining state an input vector respectively as $x = \left[L_a i_a \quad L_b i_b \quad L_c i_c \quad L_d i_d \quad j\omega\right]^T$ and using (1), then dynamic system for current loop controller design can be represented as:

$$\dot{x} = f_0(x) + g_0 u$$
$$= \begin{pmatrix} -\frac{r_k}{L_k} x_i - \frac{dL_k}{d\theta}\frac{x_i x_5}{jL_k} & ,i = 1,2,3,4. \\ \frac{1}{2}\sum_{k=a,i=1}^{d,4} \frac{dL_k(\theta, i_k)}{d\theta}\frac{x_i^2}{L_k^2} - T_L - \frac{B}{j}x_5 & \end{pmatrix}$$
$$+ \begin{pmatrix} 1 & 0 & 0 & 0 \\ 0 & 1 & 0 & 0 \\ 0 & 0 & 1 & 0 \\ 0 & 0 & 0 & 1 \\ 0 & 0 & 0 & 0 \end{pmatrix} u \tag{12}$$

For convenience, first following pre-feedback to the original system is used to simplify the controller design:

$$u_k = \frac{r_k}{L_k} x_i + \frac{dL_k}{d\theta}\frac{x_i x_5}{jL_k} + v_k \tag{13}$$

So, affine dynamic system (12) converts to:

$$\dot{x} = f(x) + g_0 v$$
$$= \begin{pmatrix} 0 \\ \frac{1}{2}\sum_{k=a,i=1}^{d,4} \frac{dL_k(\theta, i_k)}{d\theta}\frac{x_i^2}{L_k^2} - T_L - \frac{B}{j}x_5 \end{pmatrix} + gv \tag{14}$$

Obviously, achieving the regulating objective is equivalent to asymptotically stabilizing the equilibrium x^*. In order to stabilize the desired equilibrium point, one can use a Hamiltonian function as:

$$H_d(x) = \frac{1}{2}(x - x^*)^T \lambda (x - x^*)$$
$$= \frac{\lambda_1}{2}(x_1 - x_1^*)^2 + \ldots + \frac{\lambda_5}{2}(x_5 - x_5^*)^2 \tag{15}$$

The feedback law to make desired equilibrium point x^* asymptotically stable is used as:

$$v = \varphi_i(x_i) = \left(\varphi_1(x_1) \cdots \varphi_4(x_4)\right)^T \tag{16}$$

Such that $f(x) + g(x)\varphi = F_d(x)\partial H_d(x)$. Where $F_d(x)$ is a $n \times n$ dissipative matrix. According to Lemma 1, such a feedback exists if and only if (16) holds. The $F_d(x)$ matrix is chosen in order to facilitate the solution of the resulting algebraic equations. Furthermore, in order to simplify the control structure, we want to assign one output to each control action and also to obtain a controller as simpler and robust (minimum parameter dependence) as possible. In the stability analysis, the damping coefficient (which is present in all real machines) plays a fundamental role to ensure convergence to the equilibrium point. The presented method allows decoupling the outputs,

improving the robustness and facilitating the gain tuning [15]. Therefore, $F_d(x)$ matrix is chosen in order to render the resulting Hamiltonian system dissipative using (9) and facilitate the solution of the resulting algebraic equations as:

$$F_d(x)=\left(\begin{array}{cccc|c} -\Gamma_1 & 0 & 0 & 0 & -\beta_1 \\ 0 & -\Gamma_2 & 0 & 0 & -\beta_2 \\ 0 & 0 & -\Gamma_3 & 0 & -\beta_3 \\ 0 & 0 & 0 & -\Gamma_4 & -\beta_4 \\ \hline \beta_1 & \beta_2 & \beta_3 & \beta_4 & \alpha \end{array}\right) \tag{17}$$

where $\Gamma_i > 0$ are arbitrary positive constants. From (12) and assuming $B \cong 0$, a particular solution is:

$$\beta_i = \frac{x_i}{2L_k{}^2\lambda_i}\frac{dL_k}{d\theta}, \alpha = 0 \tag{18}$$

We can solve for the feedback $v = \varphi_i(x_i)$ from (10) as:

$$\varphi_i(x_i) = -\Gamma_i \frac{\partial H_d}{\partial x_i} - \frac{1}{2L_k{}^2\lambda_i}\frac{dL_k}{d\theta}x_i\frac{\partial H_d}{\partial x_5} \tag{19}$$

The resulting closed-loop system is:

$$\dot{x} = \left(J_d(x) - R_d(x)\right)\partial H_d(x) \tag{20}$$

in which

$$J_d(x) = \frac{1}{2}\left(F_d(x) - F_d{}^T(x)\right)$$

$$= \left(\begin{array}{ccc|c} & & & \frac{-x_1}{2L_a^2\lambda_1}\frac{dL_a}{d\theta} \\ & 0_{4\times4} & & \vdots \\ & & & \frac{-x_4}{2L_d^2\lambda_4}\frac{dL_d}{d\theta} \\ \hline \frac{x_1}{2L_a^2\lambda_1}\frac{dL_a}{d\theta} & \cdots & \frac{x_4}{2L_d^2\lambda_4}\frac{dL_d}{d\theta} & 0 \end{array}\right)$$

and

$$R_d = -\frac{1}{2}\left(F_d + F_d{}^T\right) = \left(\begin{array}{cccc|c} \Gamma_1 & 0 & 0 & 0 & \\ 0 & \Gamma_2 & 0 & 0 & 0_{4\times1} \\ 0 & 0 & \Gamma_3 & 0 & \\ 0 & 0 & 0 & \Gamma_4 & \\ \hline & 0_{1\times4} & & & 0 \end{array}\right) \geq 0$$

In order to prove that x^* is asymptotically stable, now calculate the derivative of $H_d(X)$ along the trajectories of the closed loop as follows:

$$\begin{aligned} \dot{H}_d &= -\left[\partial H_d\right]^T R_d \partial H_d \\ &= -\lambda_1\Gamma_1(x_1 - x_1^*)^2 - \cdots - \lambda_4\Gamma_4(x_4 - x_4^*)^2 \leq 0 \end{aligned} \tag{21}$$

Hence, $H_d(X)$ qualifies as a Lyapunov function. Closed loop system (8) with x^* (locally) stable equilibrium is asymptotically stable if, in addition, the largest invariant set under the closed–loop dynamics (8) contained in $\{x \in R^n \mid \left[\partial H_d\right]^T R_d \partial H_d = 0\}$ Equals x^*. Asymptotic stability follows immediately invoking LaSalle's invariance principle and the above condition. Finally, combining the two controls (13) and (19), it is easy to obtain:

$$\begin{aligned} u_k &= -\Gamma_i\lambda_i L_k(i_k - i_k^*) + r_k i_k - \frac{dL_k}{d\theta} i_k\,\omega \\ &\quad - \frac{1}{2L_k{}^2\lambda_i}\frac{dL_k}{d\theta} i_k\, j\lambda_5(\omega - \omega^*) \end{aligned} \tag{22}$$

4 Simulation Results

The proposed controllers are simulated using the SIMULINK software. The model takes magnetic saturation into account. The drive system simulations are used for comparison purposes to investigate the performance of the proposed PBC approach at different load conditions. From the imposed pole locations, the gains of current PI controller are computed and the damping parameter values of passivity-based controller have been obtained by using a trial-and-error procedure. The desired rotor speed is set to 200 RPM and the external load torque is suddenly changed at t=0.05 second from $5\ Nm$ to $10\ Nm$. Simulation result obtained for proposed controllers shows in Fig. 3(a) and 3(b). As it can be considered higher tracking performance of reference speed achieved in the case of using passivity-based current loop controller with adaptive sliding speed loop control.

5 Experimental Setup and Results

The validity and effectiveness of the proposed control approach are shown by adopting the same objectives as the simulation results. The controller gains are nearly the same as used in the system simulation. A DSP-based drive system using a four-phase 8/6 4KW oulton SRM which has the nonlinear static flux linkage and torque characteristics shown in Fig. 1 is used to test speed controllers experimentally. The work presented here employs a conventional digital-control platform. It is based on the eZdsp F2812 board as a suitable platform for implementing motor controllers. This board is built around the TMS320F2812 digital signal processor (DSP). This platform is compatible with Simulink, and includes four dual pulse-width-modulation (PWM) channels (8 channels total), 4

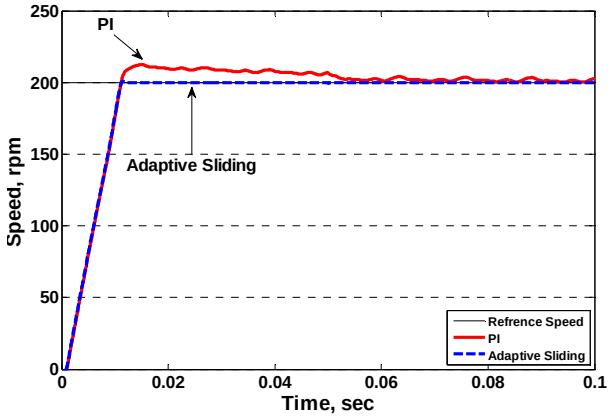

(a)

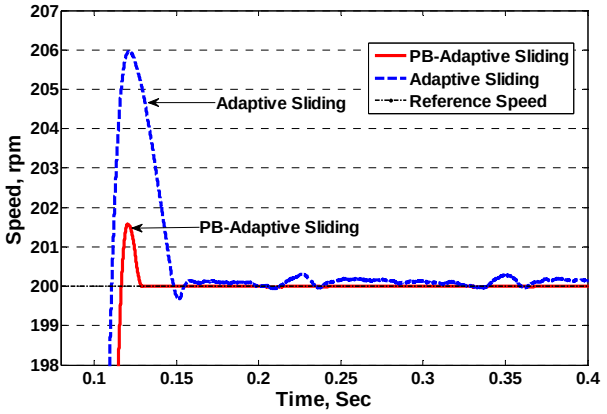

(b)

Fig. 3 (Simulation results) Motor Speed comparison. (a) Between PI and adaptive Sliding mode without using passivity-based current controller. (b) with and without using PBC technique.

analog-to-digital converters (ADCs), and a speed-encoder input. The processor is a 32-bit DSP with fixed-point arithmetic; thus, discrete and fixed-point math blocks from Simulink can be used to program it. The complete experimental hardware used for evaluating the 8/6 SRM drive is shown in Fig. 4. a conventional asymmetric converter used for our four-phase SR drive circuit. Simulink is able to compile a block diagram into C code and then call CCS to generate assembly code for the DSP. A project is generated in CCS to be loaded into the DSP. Fig. 5 shows a summary of the setup. The experimental results were obtained for the SRM speed controls shown in Fig. 6. Speed reference tracking improvement was performed through the proposed idea in 200 rpm on 5Nm load condition.

Since a torque sensor was not available, for the electromagnetic torque, only simulation results comparing the response of three controllers are presented. Fig. 7 shows that performance of electromagnetic torque has been increased to a value corresponding to the load and obviously can be observed that torque ripple associated with using passivity-based controller operation is significantly decreased. Fig. 8 shows current and voltage waveforms for case of using passivity-based adaptive sliding mode control algorithm. Experimental waveforms show an acceptable current control mode.

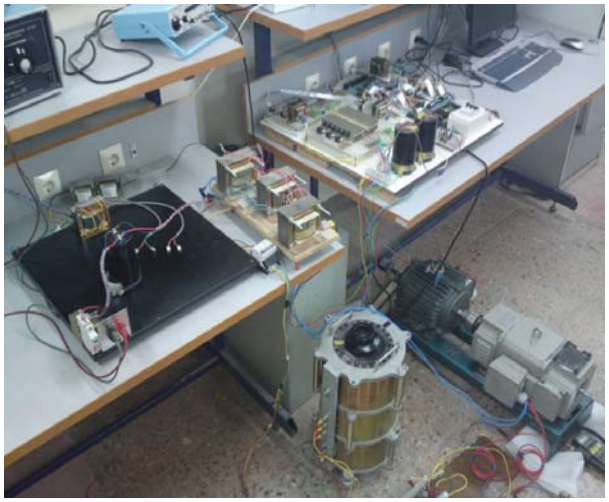

Fig. 4 SRM drive test setup used for experimentation.

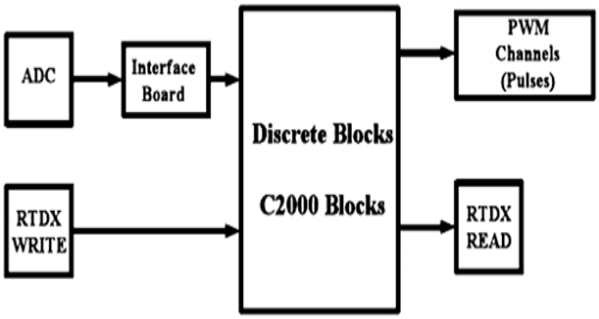

Fig. 5 Hardware and software interconnections.

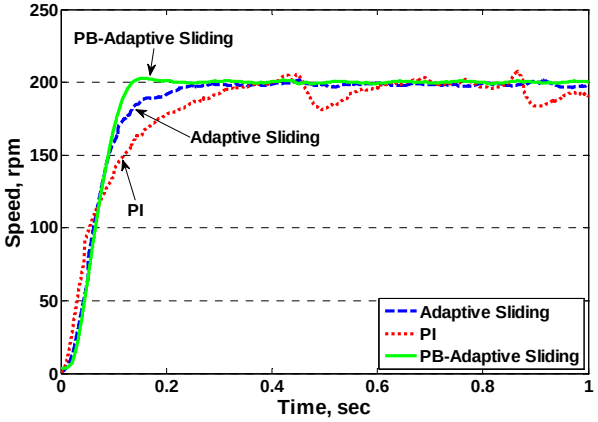

Fig. 6 (Experimental results) Speed response comparison.

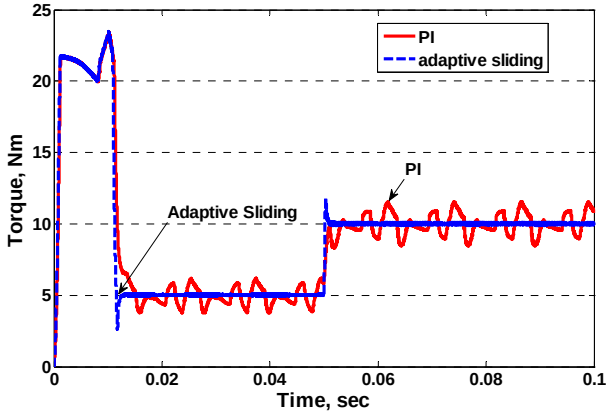

(a)

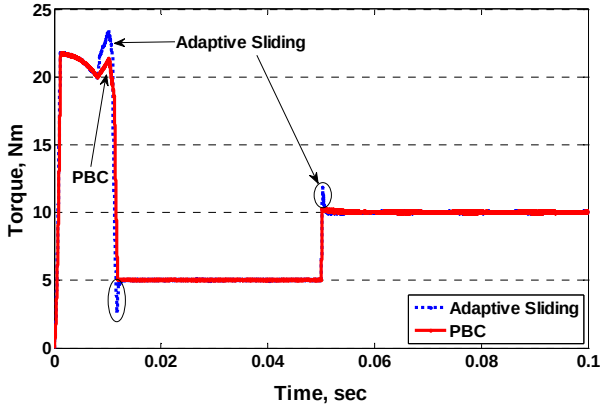

(b)

Fig. 7 SRM torque comparison of simulation results. (a) Without using PBC. (b) With using PBC.

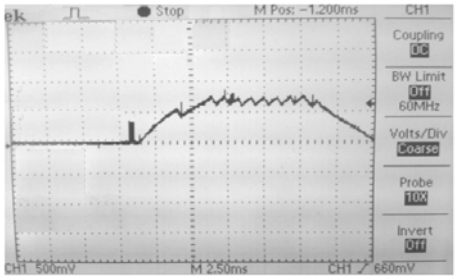

(a)

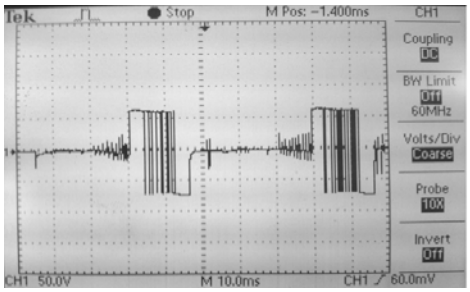

(b)

Fig. 8 Phase-one current and voltage for passivity-based adaptive sliding mode control. (a) Phase current (1.5A/div). (b) Phase voltage (50 v/div).

6 Conclusions

A nonlinear controller has been presented for a four-phase SRM drive based on the passivity-based adaptive sliding technique. Complete model of SRM possesses two-time-scale characteristics and decomposed as the feedback interconnection of the two electrical and mechanical passive linked subsystems. Hence, by using cascaded torque control structure, the proposed PBC algorithm is designed. Because of tacking the machine physical structure characteristics into account, it can overcome the inherent nonlinear characteristics of the system. The simulation and experimental results show the proposed controller has improved dynamic performance of rotor speed and torque, also produces lower torque ripple for SRM drives. The controller is not deigning to compensate for the uncertainties caused by the parameter variations and external load disturbance. Future research includes a dynamical extension keeping the Hamiltonian structure to improve the robustness (basically on the electrical parameters) and the performance.

Appendix

Table 1 Motor specifications

Rated power	4 kW
Rated phase current	9 A
Rated speed	1500 rpm
Number of pole	8/6
Phase resistance	0.75 Ω
Inertia (J)	0.008 $N.ms^2$
Damping Factor (B)	0.00078 Nms

References

[1] Krishnan R., *Switched Reluctance Motor Drives*, chapter 9, pp. 408-412, Boca Raton, FL: CRC Press, 2001.

[2] Chuang T. S. and Pollock C., "Robust speed control of a switched reluctance vector drive using variable structure approach", *IEEE Trans. on Industrial Electronic*, Vol. 44, No. 6, pp. 800-808, Dec. 1997.

[3] Cheok A. D. and Wang Z., "Fuzzy logic rotor position estimation based switched reluctance motor DSP drive with accuracy enhancement", *IEEE Trans. On Power Electronics*, Vol. 20, No. 4, pp. 908-921, July 2005.

[4] Ge B., Wang X., Su P. and Jiang J., "Nonlinear internal-model control for switched reluctance drives", *IEEE Trans. On Power Electronics*, Vol. 17, No. 3, pp. 379-388, May 2002.

[5] Feyzi M. R. and Ebrahimi Y., "Direct Torque Control of 5-Phase 10/8 Switched Reluctance Motors", *Iranian Journal of Electrical & Electronic Engineering*, Vol. 5, No. 3, pp. 205-214, Sep. 2009.

[6] Ortega R., van der Schaft A., Maschke B. and Escobar G., "Interconnection and damping assignment passivity-based control of port-controlled hamiltonian systems", *Automatica*, Vol. 38, No. 4, pp. 585–596, Sep. 2002.

[7] Sedghizadeh S., Lucas C. and Ghafoori Fard H., "Sensorless Speed Control of Switched Reluctance Motor Drive Using the Binary Observer with Online Flux-Linkage Estimation", *Iranian Journal of Electrical & Electronic Engineering*, Vol. 5, No. 2, pp. 143-150, Jun. 2009.

[8] Asgar M. and Afjei E., "A New Class of Resonant Discharge Drive Topology for Switched Reluctance Motor", *Iranian Journal of Electrical & Electronic Engineering*, Vol. 5, No. 4, pp. 261-269, Dec. 2009.

[9] Taylor D. G., "An experimental study on composite control of switched reluctance motors", *IEEE Contr. Syst. Mag.*, Vol. 11, pp. 31–36, Feb. 1991.

[10] Espinosa-Pe´rez G., Maya-Ortiz P., Velasco-Villa M. and Sira-Ramirez H., "Passivity-based control of switched reluctance motors with nonlinear magnetic circuits", *IEEE Trans. On Control System Technology*, Vol. 12, No. 3, pp 439–448, May 2004.

[11] Chen C. A., Chiang H. K. and Lin B. R., "The novel adaptive sliding mode control for current sensorless synchronous reluctance motor speed drive", *IEEE International Conference on Industrial Technology*, *ICIT*, China, pp. 1-6, April 2008.

[12] Marino R. and Tomei P., *Nonlinear Control Design*, chapter 4, pp. 272-273, Prentice Hall, Inc, 1995.

[13] Chen C. and Liu T., "Nonlinear Controller Design for Switched Reluctance Drive System", *IEEE Trans. On Aerospace And Electronic Systems*, Vol. 39, No. 4, pp. 1429-1440, Oct. 2003.

[14] Guo Y., Xi Z. and Cheng D., "Speed regulation of permanent magnet synchronous motor via feedback dissipative hamiltonian realisation", *IET Control Theory Appl.*, Vol. 1, No.1, pp. 281–290, Jan. 2007.

[15] Doria-Cerezo A., Batlle C. and Espinosa-Perez G., "Passivity-based control of a wound-rotor synchronous motor", *IET Control Theory Appl.*, Vol. 4, No.10, pp. 2049–2057, July 2010.

Mohammad Masoud Namazi Isfahani was born in Isfahan, Iran, in 1986. He received the B.Sc. degree from Shahed University, Tehran, Iran, in 2008 and the M.Sc. degree from Isfahan University of Technology, Isfahan, Iran, in 2011, where he is currently working toward the Ph.D. degree in the Department of Electrical and Computer Engineering. His fields of research are nonlinear control, electric machines modeling and variable-speed drives.

Amir Rashidi was born in Mashhad, Iran, in 1984. He received the B.Sc. degree from Sistan and Baluchestan University, Zahedan, Iran, in 2006 and the M.Sc. degree from Isfahan University of Technology, Isfahan, Iran, in 2009, where he is currently working toward the Ph.D. degree in the Department of Electrical and Computer Engineering. His research interests include electric motor drives, power electronics and microprocessor-based control systems.

Sayed Morteza Saghaian-Nejad was born in Isfahan, Iran, in 1952. He received the B.A., M.Sc. and Ph.D. degrees in Electrical Engineering from the University of Kentucky, U.S.A. in 1977, 1979 and 1989. Since 1979, he has been with the respectively Department of Electrical and computer Engineering of Isfahan University of Technology, as a faculty member, where he is currently a professor. His research interests are in the area of Electrical Machines, Power Electronics and Drives.